First Hyperpolarizability of a Sesquifulvalene Transition Metal Complex by Time-Dependent Density-Functional Theory

Wolfgang Hieringer*,† and Evert Jan Baerends*,‡

Institut für Physikalische und Theoretische Chemie, Universität Erlangen−Nürnberg, Egerlandstrasse 3, 91058 Erlangen, Germany, and Theoretische Chemie, Faculteit Exacte Wetenschappen, Vrije Universiteit Amsterdam, De Boelelaan 1083, 1081 HV Amsterdam, The Netherlands

Received: July 21, 2005; In Final Form: October 26, 2005

The first hyperpolarizability and electronic excitation spectrum of sesquifulvalene and a sesquifulvalene ruthenium complex have been computed and analyzed with use of time-dependent density-functional theory. A new orbital decomposition scheme is introduced that allows the computed first hyperpolarizability to be related to the electronic structure of complex molecules. The analysis shows that the first hyperpolarizability of sesquifulvalene is not associated with the first intense absorption, with HOMO-1 → LUMO+1 character, but is dominated by the lowest energy transition, with HOMO → LUMO character, despite its very low intensity. In the ruthenium complex, the analysis reveals that the strong enhancement of the nonlinear optical response compared to free sesquifulvalene should not be attributed to the effect of complexation on the hyperpolarizability of sesquifulvalene. The strong hyperpolarizability originates from MLCT transitions from ruthenium d-orbitals to an empty orbital located at the seven ring of sesquifulvalene, transitions that have no analogue in free sequifulvalene.

1. Introduction

The development of chromophores for nonlinear optics (NLO) has been driven by a multitude of important technological applications that can be realized if suitable materials are available.[1−3] In applications where fast nonlinear optical response is desired, molecular chromophores with high electronic nonlinear susceptibilities have been particularly promising to replace traditional materials where the nonlinear effect comes from the relatively slow response of the nuclear framework instead of electronic degrees of freedom.

The design of new chromophores with improved nonlinear optical properties has profited greatly from theoretical considerations concerning the microscopic mechanism and accurate computation of molecular hyperpolarizabilities.[4] The application of perturbation theory has led to so-called "sum-over-states" formulas, where the molecular hyperpolarizabilities are expressed as a sum of contributions from the ground and excited states of the system.[5,6] A drastic simplification of these expressions, the so-called "two-level formula" (eq 1), where the abovementioned sum is truncated to include only the ground state and a single excited state as the leading contribution, has been particularly useful for the development of new chromophores.

$$\beta \propto \frac{\Delta\mu_{ge}\cdot\mu_{ge}^2}{\Delta E_{ge}^2} \qquad (1)$$

In eq 1, β denotes the static first hyperpolarizability, ΔE_{ge} denotes the excitation energy separating the ground and excited state, $\Delta\mu_{ge}$ denotes the difference in dipole moments of the ground and excited state, and μ_{ge} is the transition dipole moment of the excitation, which is related to its optical intensity. Hence, as a guideline, the two-level formula suggests building chromophores with at least one low-energy, high-intensity charge-transfer excitation.[4,7] Later on, more sophisticated approximate analysis tools such as the "missing-state analysis"[8] or the "missing-orbital analysis",[9] where individual states are deleted from the full sum-over-states expression to estimate their importance, have been proposed to obtain more insight into the origins of the hyperpolarizabilities of complex molecules. However, the success of the simple two-level formula has never been reached by other approaches since, and in fact it still seems to be the most important design rule for chromophore synthesis in practical use.

Figure 1. Most important resonance structures of sesquifulvalene **1**.

In recent years, a great number of organic and organometallic chromophores for NLO have been synthesized, some of which show extremely high hyperpolarizabilities. The latter class of compounds offers additional flexibility due to the presence of transition metals.[10,11] Most of the successful NLO chromophores show a push−pull architecture as a common structural motif, i.e., they contain an electronic donor group (such as $-NH_2$) and an electronic acceptor group (such as $-NO_2$) connected by a bridge (such as ethylene or benzene) to mediate the electronic communication between the two groups.

Sesquifulvalene **1** represents a push−pull architecture, as becomes clear from the resonance structures drawn in Figure 1, and theoretical investigations predicted considerable optical nonlinearities.[12−14] However, sesquifulvalene itself is unsuitable for the construction of NLO materials due to its high chemical reactivity, which is probably the reason its hyperpolarizabilities have never been measured experimentally to our knowledge.

* To whom correspondence should be addressed. E-mail: hieringer@chemie.uni-erlangen.de, baerends@few.vu.nl.
† Universität Erlangen−Nürnberg.
‡ Vrije Universiteit Amsterdam.

10.1021/jp0540297 CCC: $33.50
Published on Web 12/24/2005

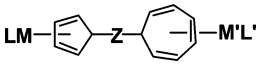

Figure 2. General structure of sesquifulvalene transition metal complexes: Z, conjugated bridge; LM, M′L′, transition metal complex fragments.

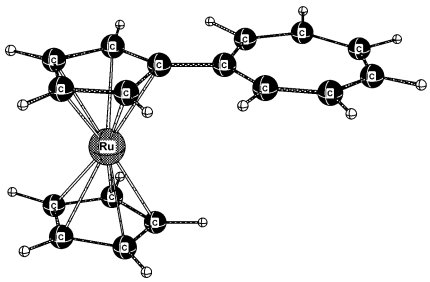

Figure 3. The title sesquifulvalene complex **2**.

On the other hand, **1** forms stable organometallic coordination compounds upon complexation with various transition metal fragments. In the groups led by Heck and by Tamm, various sesquifulvalene transition metal complexes (for a general formula cf. Figure 2) have been synthesized, and their first hyperpolarizabilities have been measured by means of Hyper−Rayleigh scattering[15,16] experiments.[17−22] Some of the hyperpolarizabilities reported are quite high compared to those of chromophores of comparable molecular size. To better understand the origins of the observed hyperpolarizabilities, various experimental techniques have been applied to elucidate the electronic structure of the compounds.[17] In particular, the two-level formula has been applied to obtain an estimate for the static (i.e., frequency-independent) first hyperpolarizabilities from the experimentally accessible frequency-dependent hyperpolarizabilities. A knowledge of the static hyperpolarizability is important to assess the intrinsic capabilities of a chromophore for NLO applications in various experimental setups.

In this contribution, we present a theoretical analysis of the fist hyperpolarizabilities of sesquifulvalene **1** and its prototype ruthenium sandwich-type complex **2**, shown in Figure 3, using time-dependent density-functional calculations.[23] Our main goal is to contribute to a better qualitative understanding of the observed first hyperpolarizabilities. In particular, we will shed some light on the effect of complexation on the hyperpolarizability of the sesquifulvalene ligand. To this end, we propose a new approximate analysis scheme based on response theory, which provides a convenient way to relate the computed first hyperpolarizabilities to the details of the electronic structure of complex chromophores. We will investigate the properties of the new scheme by analyzing the well-known NLO chromophore *p*-nitroaniline (PNA), and subsequently apply the method to better understand the NLO properties of sesquifulvalene **1** and its complex **2**.

The paper is organized as follows. In Section 2, we start with some computational details, and outline the basic equations of the new approximate orbital decomposition scheme for first hyperpolarizabilities. In Section 3.1, some information is given on the geometrical features of the title compounds. This section is followed by an analysis of the electronic structure and excitation spectrum, and in Section 3.3 we elaborate on the hyperpolarizabilities of sesquifulvalene and the title complex.

2. Methods

2.1. General. The electronic excitation energies and frequency-dependent first hyperpolarizabilities were calculated analytically by using time-dependent density-functional theory (TDDFT)[24−28] as implemented into the Amsterdam Density Functional program (ADF).[23,29] Both the static hyperpolarizabilities and those at an incident frequency of 0.043 au, which is the laser frequency used in the experiments (1064 nm),[17] have been computed. The algorithms used and the implementation have been described in detail elsewhere.[30]

In the ground-state self-consistent-field calculations preceding the TDDFT steps, exchange-correlation (xc) potentials based on the local density approximation (LDA)[31,32] and the gradient-regulated connection (GRAC)[33] of the potentials based on the exchange-correlation functional proposed by Becke[34] and Perdew[35] and the shape-corrected LB94 potential due to van Leeuwen and Baerends[36] have been used. The SCF procedure was converged below 10^{-8} au, and the integration accuracy parameter was set to 5. For the subsequent TDDFT computations, the adiabatic exchange-correlation kernel based on the local density approximation (ALDA) has been used along with both the LDA and the GRAC potential.

For the response calculations, we have tested Slater-type basis sets of varying quality. In particular, basis sets including diffuse functions are generally believed to be important for accurate excitation energies and hyperpolarizabilities of small molecules. On the other hand, the presence of very diffuse atom-centered basis functions in larger molecules may lead to numerical problems due to linear dependencies and concomitant deterioration of the results.[37] In the present case, we have found that the inclusion of diffuse basis functions is not of crucial importance for the calculated hyperpolarizabilities as long as one is only interested in qualitative results. This may be expected for somewhat larger and/or cationic molecules such as those investigated here. Moreover, since accurate (experimental or correlated ab initio) gas-phase hyperpolarizabilities for comparison with our TDDFT results are lacking presently, there is no need to push basis set issues to the limit. We have therefore chosen to base our study on standard basis sets of polarized triple-ζ quality.

All geometries were fully optimized in C_{2v} (sesquifulvalene **1**) and C_s (complex **2**) symmetry at the BP86/TZ2P or BP86/TZP level,[34,35] using version 2000.1 of the ADF program. The computed hyperpolarizabilities have been analyzed in a semiquantitative manner by virtue of a orbital decomposition scheme, which will be described in the following section. The scheme has been implemented in a local version of the ADF program based on release 2000.1

2.2. Orbital Decomposition Scheme for First Hyperpolarizabilities. Explicit expressions for the computation of first hyperpolarizabilities within time-dependent Hartree−Fock (TDHF) theory have been given by Sekino and Bartlett[38] and by Karna and Dupuis.[39] The decomposition scheme to be presented is based on the expression for the hyperpolarizability tensor element β_{abc} given in ref 39, see eq 2.

$$\beta_{abc} = Tr[\mathbf{n}\mathbf{U}^a\mathbf{G}^b\mathbf{U}^c] - Tr[\mathbf{n}\mathbf{U}^a\mathbf{U}^c\epsilon^b] = 2\sum_{i}^{\mathrm{occ}}\sum_{k}^{\mathrm{virt}}\sum_{l}^{\mathrm{virt}} U_{ik}^a\, G_{kl}^b\, U_{li}^c - 2\sum_{i}^{\mathrm{occ}}\sum_{k}^{\mathrm{virt}}\sum_{l}^{\mathrm{occ}} U_{ik}^a\, U_{kl}^c\, \epsilon_{li}^b \quad (2)$$

The definition of the occupation number matrix **n**, the first-order Fock matrix $\mathbf{G}^b$, the Lagrangian multiplier matrix ϵ^b, and the transformation matrix $\mathbf{U}^a$ follow that in ref 39. (Upper indices indicate perturbed quantities to first order in the external electric field.)

Van Gisbergen, Snijders, and Baerends have extended these equations to the realm of DFT, which includes a contribution to the hyperpolarizability originating from the expansion of the

exchange-correlation contribution in terms of the external electric field and which are not present in TDHF theory.[23] In practice, it turned out that this contribution is small in magnitude (<5%, usually even <1%) for most molecules. Although this extra DFT term is of course included in the calculated hyperpolarizabilities given in this paper, it is omitted from the orbital decomposition scheme to be outlined here. It implicitly enters into the expression, however, since it is included in the determination of the matrixes **U** and **G** within the coupled-perturbed Kohn−Sham (CPKS) scheme. The decomposition scheme yields qualitative or at best semiquantitative information, and the approximation of omitting the small g_{XC} terms will not affect the insights obtained.

In the orbital decomposition scheme to be presented, the contributions of individual orbitals and orbital groups (pairs) to any total hyperpolarizability tensor element β_{abc} is identified and used as a tool to relate the computed hyperpolarizability to the electronic structure of the molecule at hand. To this end, starting from the general expression in eq 2, the contribution of a particular orbital pair characterized by indexes i, r, $\beta_{abc}(i,r)$ to a given hyperpolarizability tensor element β_{abc} (static or frequency-dependent) is expressed by defining the corresponding restricted sum as given in eq 3.

$$\beta_{abc}(i,r) = 2\Big(\sum_{s}^{\text{virt}} U_{ir}^{a}\, G_{rs}^{b}\, U_{si}^{c} + \sum_{s}^{\text{virt}} U_{is}^{a}\, G_{sr}^{b}\, U_{ri}^{c}\Big) - 2\Big(\sum_{j}^{\text{occ}} U_{jr}^{a}\, U_{ri}^{c}\, \epsilon_{ij}^{b} + \sum_{j}^{\text{occ}} U_{ir}^{a}\, U_{rj}^{c}\, \epsilon_{ji}^{b}\Big) \quad (3)$$

This results in a decomposition of a given (static or frequency-dependent) hyperpolarizability tensor element β_{abc} into contributions by occupied-virtual orbital pairs $\beta_{abc}(i,r)$.[41] (An extension to combinations of one occupied orbital with two virtual orbitals $\beta_{abc}(i,r,s)$ is straightforward but not used here).

Note that only the full sum, eq 2, for the tensor element β_{abc} has a physical meaning in describing the response of the dipole moment to second order in the external electric field, leaving aside the extra DFT term as explained above. The contributions of the individual orbital groups (eq 3) in total add up to this number. Thus, it may happen that certain terms in the above sum cancel other contributions with opposite sign. In cases where major contributions to β_{abc} are canceled in this way, the use of the analysis scheme may be questionable. These considerations have been taken into account in the analyses given in later sections of the present paper.

At this point, we stress the relation of this approach, which is based on response theory, to analysis tools using sum-over-states expressions[40,42] which allows for the identification of those excitations which contribute most to the total β tensor element (missing state analysis,[8] missing orbital analysis[9]). The disadvantage of the latter approaches is that all electronic excited states have to be calculated to obtain an exact decomposition, which is usually affordable for semiempirical methods only. The present scheme, on the other hand, is obtained as a byproduct of the calculation of the total hyperpolarizability tensor and comes at virtually no additional cost in computer or human user time.

We will demonstrate the properties of the present decomposition scheme in Section 3.3.1 by analyzing the well-known NLO chromophore *p*-nitroaniline (PNA) as an example. There, the following basis sets have been used to establish the stability of the scheme with respect to basis set variations. In addition to the standard TZ2P basis set, several basis sets have been tested where the exponents have been obtained from an even-tempered series. The label DZPhp refers to an even-tempered basis set of polarized double-ζ split-valence quality, augmented with several diffuse functions (e.g., 3S 3P 2D 1F for carbon). The labels VI and VII refer to very extensive polarized even-tempered split-valence basis sets (for carbon: 6S 4P 2D 1F for VI, 8S 6P 3D 2F for VII), which are augmented by several diffuse functions in the case of VIhp (+ 2S 2P 2D 3F) and VIIhp (+ 1S 1P 1D 3F). In case of linear dependencies of the basis sets, certain symmetrized fragment orbitals have been removed from the molecular basis to avoid numerical problems. The shape-corrected exchange-correlation potentials SAOP[43] and GRAC[33] have been used in addition to the local density approximation (LDA).

TABLE 1: Bond Distances (in pm) of 1 and 2 at the BP/TZ2P (1, C_{2v}) and BP/TZP (2, C_s) Levels of Theory, Respectively[a]

structural parameter	1	2
C1−C2 (5-ring of Sq)	145.8	145.7
C2−C3	137.1	142.2
C3−C4	145.3	143.3
C1−C1′ (central bond in Sq)[b]	140.0	144.9
C1′−C2′ (7-ring of Sq)	144.8	143.1
C2′−C3′	136.8	138.2
C3′−C4′	143.4	141.9
C4′−C5′	136.6	138.2
Ru−C1		223.2
Ru−C1′ [b]		317.1

[a] Sq: sesquifulvalene subunit in **1** and **2**. [b] Crystal structure data for **2**: 147.2(7) pm for C1−C1′, 311.3(5) pm for Ru−C1′.[17]

3. Results and Discussion

3.1. Structural Features. The general structural features of sesquifulvalene **1** have been discussed in considerable detail before[12−14] so that we can focus on the most important features of relevance for the present study. Salient structural parameters due to our calculations of sesquifulvalene and the title complex are given in Table 1.

Sesquifulvalene **1** shows a planar equilibrium structure (symmetry C_{2v}) with alternating short and long bonds, typical for a nonaromatic polyene with partial double and single bonds. This bond-length alternation within the sesquifulvalene ligand is reduced for complex **2**, where the C−C bond length pattern indicates a partially biaromatic electronic structure with coplanar rings, with clearly increased aromatic character in particular in the 5-ring, and a lengthened central bond with similar "aromatic" length. The structural parameters for the complex are in reasonable agreement with those deduced form X-ray diffraction data.[17]

3.2. Electronic Structure and Electronic Excitation Spectrum. *3.2.1. Electronic Structure.* Although details of the electronic structure of sesquifulvalene have been studied in the literature before,[12−14] we review some important results here since this will be necessary for our analysis of the complex **2** given in the next section. Figure 4 shows the relevant frontier orbitals of sesquifulvalene along with their formal construction from cyclopentadienyl and cycloheptatrienyl fragment orbitals. Only orbitals of π-symmetry are discussed here.

According to our analysis, the HOMO of **1** belongs to the a_2 irreducible representation of the molecular point group, and is entirely located on the five-membered ring (as has already been deduced from experimental data[17]). The LUMO is also of a_2 symmetry, but resides entirely on the seven-membered ring. The π-bonding interaction of the central bond linking the two rings

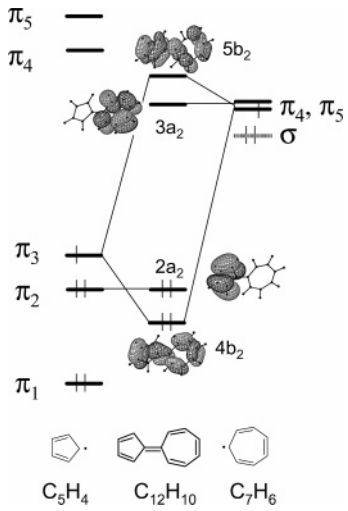

Figure 4. Four frontier orbitals and π-bonding in sesquifulvalene **1**.

can be characterized by the bonding HOMO-1 and antibonding LUMO+1 orbitals (both b_2 irrep.). We will see that these four orbitals will be of importance for the analysis of the complex in terms of electronic structure and hyperpolarizability.

The Mulliken charges of the five carbon atoms and the four hydrogen atoms constituting the five-membered ring of **1** sum up to −0.174 e in our calculations. This indicates a fairly low ionicity in the ground state, which is consistent with the polyene structure of the molecule. On the other hand, it has been suggested[17] that the electronic structure of the first *excited* state can be qualitatively described as an ionic, biaromatic resonance structure with a negative charge on the five-membered ring and a positive charge on the seven-membered ring, thus indicating a flow of negative charge from the seven-membered ring to the five-membered ring upon excitation. This view is not supported by our calculations, however. As is clearly seen from Figure 4, an excitation corresponding to the HOMO → LUMO ($2a_2 \rightarrow 3a_2$) orbital transition would relocate negative charge form the five-membered ring ($2a_2$) to the seven-membered ring ($3a_2$). When considering the (HOMO-1) → (LUMO+1) ($4b_2 \rightarrow 5b_2$) orbital transition, the charge transfer is still in the same direction, i.e., from the five-membered ring to the seven-membered ring, although much less pronounced, since a closer analysis of the orbital compositions, which are illustrated only qualitatively in Figure 4, shows that the $4b_2$ orbital (HOMO-1) is composed of 54% of a five-membered-ring fragment orbital (π_3 in cyclopentadienyl), while the $5b_2$ orbital (LUMO+1) contains 60% of a seven-membered-ring fragment orbital (π_4 in cycloheptatrienyl). Hence, our analysis does not support the simple picture of a zwitterionic excited-state model with negative charge on the five-membered ring of sesquifulvalene.

On the other hand, for the sesquifulvalene transition metal complexes, in ref 17 it is assumed that complexation increases the contribution of the bipolar resonance structure in the ground state. Transitions that are important for the hyperpolarizability are therefore viewed in ref 17 as starting from the five-membered ring of sesquifulvalene or from the whole metal−bicyclopentadienyl moiety as the donor, and arriving at the seven-membered ring as the acceptor. Without involving this change in the electronic structure of complexed sesquifulvalene as compared to free sesquifulvalene, but assuming that the complexation would leave the sesquifulvalene electronic structure relatively undisturbed, we note that a transition of mostly sesquifulvalene $2a_2 \rightarrow 3a_2$ (Figure 4) character would conform to such a donor−acceptor denotation. Hence, the view taken in ref 17 for the transition metal sesquifulvalene complexes conforms to our analysis of free sesquifulvalene. Only the charge rearrangement assumed in ref 17 for the free sesquifulvalene does not conform to our analysis of the same molecule. A more complete characterization of the electronic excitations in **1** and **2** based on TDDFT calculations will be given in the next section.

We are now going to address the question of how the electronic structure changes when a cyclopentadienyl−ruthenyl $[(C_5H_5)Ru]^+$ fragment is coordinated to the sesquifulvalene ligand. To this end, the electronic structure of the cationic complex **2**, which has not been fully analyzed before, will be discussed in some detail.

The right-hand side of Figure 5 schematically shows the relevant frontier orbital energy levels of the sesquifulvalene complex. The observed pattern can be rationalized based on the well-known orbital energy level diagram of ruthenocene, given on the left-hand side of Figure 5, and the sesquifulvalene levels shown in Figure 4. The frontier orbitals of ruthenocene

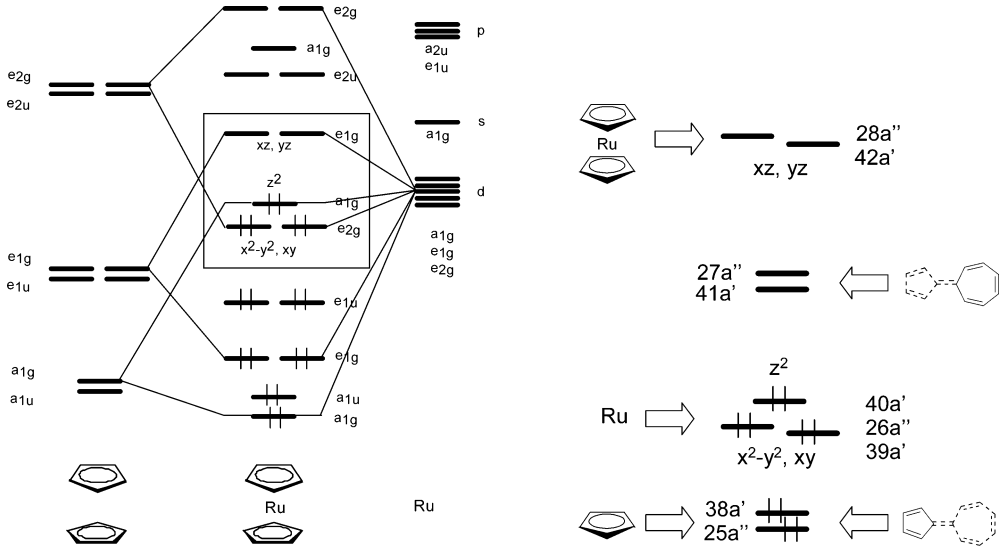

Figure 5. Qualitative frontier molecular orbital energy diagrams of ruthenocene (left) and the sesquifulvalene complex **2** (right). In the right diagram, arrows qualitatively indicate which fragments contribute to the relevant molecular orbital of **2**. The splitting of the d-levels of the ruthenium fragment is the same as that of ruthenocene (boxed area in the left diagram). The arrows on the right side indicate where the sesquifulvalene levels (cf. Figure 4) enter.

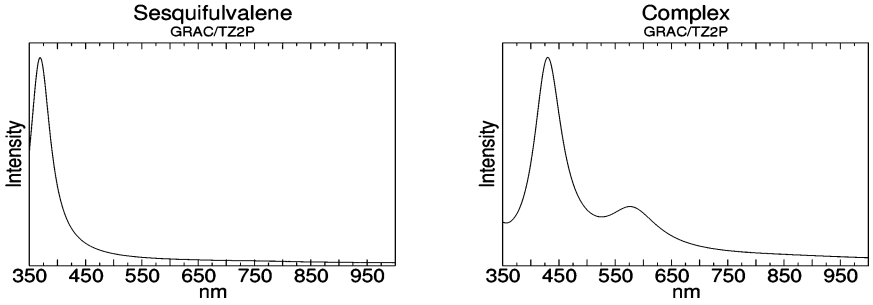

Figure 6. Simulated electronic excitation spectra of **1** (left panel) and **2** (right panel), based on electronic excitations computed at the GRAC/TZ(2)P level; all computed excitations in the energy range were included, Lorentzian line broadening of 0.4 eV fwhm was assumed; the abscissa is the wavelength [in nm]; arbitrary units for intensity.

TABLE 2: Most Intensive Excitations and Oscillator Strengths of 1 and 2 within the Range between 1.2 and 3.5 eV (350−1000 nm), Computed at the GRAC/TZ(2)2P Level (no solvent included); Projection on Single-Particle Excitations

compd	excitation	oscillator strength	projection
1	3.4 eV (370 nm)	0.69	$4b_2 \rightarrow 5b_2$ (91%)[b]
2[a]	2.1 eV (580 nm)	0.07	39a′ → 41a′ (73%), 38a′ → 41a′ (17%)
2[a]	2.9 eV (430 nm)	0.33	38a′ → 41a′ (75%), 39a′ → 41a′ (14%)
2	3.9 eV (315 nm)	0.13	37a′ → 41a′ (60%), 24a″ → 27a″ (14%)

[a] UV/vis data λ_{max} (ϵ) on **2** in solution (CH_2Cl_2): 560 nm (7360), 410 nm (14020). [b] HOMO-1 → LUMO+1.

have dominant ruthenium d-orbital character, and are split into a set of three doubly occupied orbitals and another set of two unoccupied orbitals. These orbitals, including the splitting pattern just described, can be recovered in the sesquifulvalene complex as indicated in the right panel of Figure 5 (arrows on the left-hand side with Ru or $RuCp_2$ labels). In an alternative point of view, setting out from the sesquifulvalene frontier orbitals schematized in Figure 4, the three occupied d levels (39a′, 26a″, 40a′) of the RuCp fragment energetically take a position within the HOMO−LUMO gap of sesquifulvalene, cf. right panel of Figure 5. The orbital energy levels labeled 41a′ and 27a″ have dominant sesquifulvalene seven-membered-ring character. 41a′ can be viewed as a descendant from the $5b_2$ (LUMO+1) orbital in **1**, but its weight in the seven-membered ring has increased from about 60% in **1** to 72% in **2**. The orbitals labeled 25a″ and 38a′ have significant amplitude on the five-membered ring of the sesquifulvalene ligand and the cyclopentadienyl ring attached to the ruthenium center. Hence, in the sesquifulvalene complex **2**, the HOMO (as well as HOMO-1 and HOMO-2) has predominantly ruthenium d-character, while the LUMO (41a′) is largely located on the seven-membered ring of the sesquifulvalene ligand. We will show in Section 3.3 that the nonlinear optical properties of the sesquifulvalene complex can be rationalized by the orbital energy levels shown in Figure 5.

3.2.2. Vertical Excitation Energies. The computed electronic excitation spectrum of sesquifulvalene **1** (cf. Table 2 and Figure 6, left panel) is dominated by a single intensive transition at 3.4 eV (370 nm), which corresponds mainly to the (HOMO-1) → (LUMO+1) ($4b_2 \rightarrow 5b_2$; cf. Figure 4) transition within the single-particle picture (91% contribution to the TDDFT solution vector[26]). We also note that the lowest excitation of the molecule at 1.64 eV, which corresponds to the HOMO → LUMO ($2a_2 \rightarrow 3a_2$) orbital transition, has a very low oscillator strength ($I = 0.0028$) and is therefore not shown in Table 2. The low intensity of this transition is due to a small dipole matrix element, which results from the spatial separation (poor overlap) of HOMO and LUMO in **1** (cf. Figure 4). All other excitations are computed to have lower intensities, and are therefore not discussed here.

UV/vis spectral data on complex **2** in solution have been reported by Heck et al.[17] We review the most important results derived from these experimental data before discussing our computed gas-phase spectrum. The low-energy part of the experimental UV/vis spectrum of **2** in solution is characterized by two intensive excitations within the range between 350 and 1000 nm. In the spectrum (solvent dichloromethane, CH_2Cl_2), absorption band maxima have been found at 410 and 560 nm.[17] The former, very intensive band has been assigned to an intraligand charge-transfer (LL-CT) excitation, while the latter, less intensive band has been attributed to a donor−acceptor charge-transfer (DA-CT) band.[17]

The TDDFT gas-phase spectrum of complex **2** is also shown in Figure 6 (right panel). In agreement with the experimental findings, we find two intensive transitions in the simulated spectrum within the experimentally relevant energy range. At an excitation energy of 2.1 eV (580 nm), we compute the second-most intensive excitation in the spectrum in the same energy range. This excitation is a metal-to-ligand charge-transfer (ML-CT) excitation in character, since it involves a major single-particle contribution involving an excitation from an occupied ruthenium d-orbital (39a′) to the LUMO of the complex (41a′, Table 2). The most intensive transition is found at a somewhat higher energy of 2.9 eV (430 nm). An analysis of the corresponding TDDFT solution vector reveals that this transition involves a charge transfer from orbitals located on the two five-membered rings bound to the ruthenium center to the LUMO, which is an unoccupied orbital of π-symmetry at the seven-membered ring of the ligand (descendant of the $5b_2$ orbital of **1**). We furthermore report another intensive excitation at 3.9 eV (315 nm), which is just outside the energy range of the experimental UV/vis spectrum. Higher energy excitations have not been identified experimentally, so we skip the computational results on them for conciseness.

In summary, it can be seen that the qualitative features of the experimental spectrum are well reproduced in the computations. The spectrum of **1** exhibits a very intensive transition (from HOMO-1 to LUMO+1), which shifts to lower energy upon complexation resulting in compound **2**. Just from the inspection of the optical spectra thus an enhanced hyperpolarizability of complex **2** compared to **1** may be anticipated. We will, however, demonstrate below that these intense transitions

TABLE 3: Orientationally Averaged First Hyperpolarizabilities $\bar{\beta}$ and Dominant Tensor Element β_{zzz} of *p*-Nitroaniline (PNA), Using Different Basis Sets and Exchange-Correlation Potentials (in au)[a]

			contribution to β_{zzz} (% of β_{zzz})	
level of theory	$\bar{\beta}$	β_{zzz}	HOMO ↔ LUMO	HOMO ↔ LUMO+1
LDA/TZ2P	1007	−1890	−2187 (116%)	+133 (7%)
LDA/VI	965	−1808	−2118 (118%)	+140 (8%)
LDA/VII	994	−1867	−2184 (118%)	+173 (9%)
LDA/VIhp	977	−1844	−2187 (119%)	+188 (10%)
LDA/VIIhp	985	−1851	−2185 (119%)	+178 (10%)
LDA/DZPhp	986	−1851	−2196 (119%)	+189 (10%)
GRAC/TZ2P	975	−1851	−2167 (118%)	+133 (7%)
GRAC/VIIhp	984	−1852	−2198 (119%)	+190 (10%)
GRAC/DZPhp	974	−1829	−2173 (120%)	+181 (10%)
SAOP/TZ2P	1007	−1877	−2122 (114%)	+125 (7%)
SAOP/VIIhp	975	−1819	−2100 (116%)	+148 (8%)
SAOP/DZPhp	968	−1804	−2085 (116%)	+147 (8%)

[a] Decomposition into contributions from orbital pairs; only contributions >5 % to β_{zzz} are included. The labels for the theoretical level (column 1) are explained in Section 2.

are not the primary cause of the hyperpolarizabilities, neither for **1** nor for **2**.

3.3. First Hyperpolarizabilities. *3.3.1. Orbital decomposition analysis of p-Nitroananiline.* To demonstrate that the orbital decomposition scheme for first hyperpolarizabilities may indeed be useful for qualitative and semiquantitative analysis purposes, we first apply it to a well-known chromophore for nonlinear optics, *p*-nitroaniline (PNA). The origin of the first hyperpolarizability of this molecule has been analyzed by application of various techniques (including missing-state and missing-orbital analysis schemes) before.[8,9] We will show here that the conclusions of earlier studies are qualitatively reproduced by the present decomposition scheme.

Table 3 shows the static first hyperpolarizabilities of PNA calculated by using TDDFT in combination with various exchange-correlation potentials and basis sets, cf. Section 2. Both the dominant tensor element, β_{zzz}, and the orientationally averaged hyperpolarizability, $\bar{\beta}$, are included. Furthermore, the orbital decomposition of β_{zzz} is given by using the present decomposition scheme. The data show that β_{zzz} agrees to within approximately 5% among all exchange-correlation potentials and basis sets in this case. The orbital decomposition analysis attributes a dominant role to the HOMO and LUMO, with a minor contribution (7−10%) from the HOMO−(LUMO+1) pair. Taken on its own, the former pair can be seen to overestimate the hyperpolarizability to some extent. This is partly corrected for by the latter orbital pair, however. The remaining part of β_{zzz} is compensated for by contributions of orbital pairs, the magnitude of which is less than 5% each (not shown). All other orbital pairs contribute less than 5% (positive or negative sign), and are therefore not shown. The crucial role of HOMO and LUMO for the hyperpolarizability, along with smaller correction by other orbitals, perfectly meets qualitative expectations drawn earlier from sum-over-states analysis schemes.[8,9] It can also be seen that, at least in the case of PNA, the results of the decomposition analysis appear not to be very sensitive with respect to basis sets and exchange-correlation treatment, which is convenient if qualitative conclusions are to be drawn.

*3.3.2. The Sesquifulvalene Compounds **1** and **2**.* Table 4 shows the static and frequency-dependent hyperpolarizabilities (orientationally averaged, $\bar{\beta}$, and dominant tensor element β_{zzz}) of the title compounds **1** and **2** as calculated with the methods outlined in Section 2. For the sake of better comparability, we also include corresponding numbers for PNA which have been calculated at the same level of theory.

The static first hyperpolarizability (both $\bar{\beta}$ and β_{zzz}) of the free sesquifulvalene ligand **1** is calculated at approximately one-third in magnitude of the corresponding numbers for the reference compound PNA. Complexation of sesquifulvalene with a cationic cyclopentadienyl ruthenium ($RuCp^+$) fragment, thus forming **2**, results in more than a 5-fold increase in hyperpolarizability compared to the free ligand, surpassing that of PNA by a factor of 1.8 for $\bar{\beta}$. For all molecules investigated here, the numbers for the frequency-dependent second-harmonic generation (SHG) hyperpolarizabilities are quite different from the static ones. Such resonance enhancement may be expected since the photon energy of the frequency-doubled light (2.34 eV, 534 nm wavelength) is fairly close the true vertical excitation energies of the molecules (cf. Figure 6 and Table 2).

TABLE 4: Orientationally Averaged First Hyperpolarizability $\bar{\beta}$ and Largest Tensor Element β_{zzz} of 1, 2, and PNA, LDA/DZPhp[a]

	$\bar{\beta}$		β_{zzz}	
compd	static	SHG	static	SHG
1	−229	+591	−533	+723
2	−1898	−1001	−3202	−1427
PNA[b]	+986	+2235	−1851	−4004

[a] Static ($\omega = 0$) and second-harmonic generation (SHG, input frequency $\omega_0 = 0.043$ au, or 1.17 eV incident photon energy); $\bar{\beta}$, β_{zzz} in au. [b] *p*-Nitroaniline.

To rationalize these computational results, we use the orbital decomposition scheme outlined in Section 2.2 to relate the dominant tensor elements β_{zzz} of the calculated first hyperpolarizabilities to the electronic structure of **1** and **2**. The decomposition scheme affords a breakdown of a chosen hyperpolarizability tensor element into contributions of individual pairs of molecular orbitals. It may thus give an indication of which parts of a chromophore molecule are directly involved in generating the observed nonlinear response.

The results of the analysis are given in Table 5. Cf. also the orbital energy level diagrams in Figure 4 and Figure 5. For a comparison with PNA, cf. Table 3.

The decomposition of the dominant hyperpolarizability tensor element β_{zzz} for the free sesquifulvalene ligand **1** singles out the contribution from the HOMO ($2a_2$) and LUMO ($3a_2$) as the most important contribution to β_{zzz}. In fact, however, this contribution actually overshoots the total β_{zzz} significantly. As can be seen from Table 5, this exaggeration is compensated for by several contributions from other orbital pairs, some of which lie in the frontier orbital region energetically, while others include high-lying virtual orbitals. In view of the low intensity of the electronic excitation dominated by the $2a_2 \rightarrow 3a_2$ transition (cf. Section 3.2.2), it is striking that the decomposition singles

TABLE 5: Orbital Decompositions of the Dominant Tensor Element β_{zzz} of the Static First Hyperpolarizability of 1 and 2 (in au); LDA/DZPhp Level of Theory

occupied ↔ virtual	contribution (% of β_{zzz})
1: $\beta_{zzz} = -533$	
$2a_2$ (HOMO) ↔ $3a_2$ (LUMO)	−890 (167%)
$2a_2$ (HOMO) ↔ $5a_2$ (LUMO+2)	+82 (15%)
$4b_2$ (HOMO-1) ↔ $12b_2$	+154 (29%)
$4b_2$ (HOMO-1) ↔ $23b_2$	+91 (17%)
$3b_2$ (HOMO-2) ↔ $5b_2$ (LUMO+1)	+54 (10%)
2: $\beta_{zzz} = -3202$	
37a′ ↔ 41a′	+181 (6%)
38a′ ↔ 41a′	−695 (22%)
39a′ ↔ 41a′	−1332 (42%)
26a″ ↔ 27a″	−702 (22%)
40a′ ↔ 41a′	−603 (19%)

out the $2a_2 \leftrightarrow 3a_2$ orbital pair as the dominant contributor to β_{zzz}. On the other hand, the $4b_2 \leftrightarrow 5b_2$ orbital pair, the corresponding electronic excitation of which has high oscillator strength (cf. Table 2), appears to contribute less than 10% (therefore not shown in Table 5). A closer analysis of the contribution due to these orbital pairs reveals that the first and second terms in eq 2 have opposite signs for the $4b_2 \leftrightarrow 5b_2$ pair and thus cancel, while they have the same sign for the $2a_2 \leftrightarrow 3a_2$ pair. Overall, the decomposition is rather complicated in this case and provides only a rough picture of the mechanism of the nonlinear response of **1**. This may be related to the fact that the total hyperpolarizability of **1** is rather small in magnitude. We note that there are sizable contributions due to $4b_2 \leftrightarrow 12b_2$, $4b_2 \leftrightarrow 23b_2$ orbital pairs, for which we have no explanation.

The analysis of the title complex **2** reveals major (>5%) contributions from five orbital pairs, cf. Table 5. In this case, all of the orbitals involved in significant contributions to β_{zzz} are close to the HOMO−LUMO gap energetically, resulting in a more consistent picture than for **1**. Considering the analysis of the electronic structure given in Section 3.2, we have identified orbitals 38a′ and 41a′ as having significant sesquifulvalene character. Table 5 shows that this orbital pair accounts for about 22% of the total β_{zzz} tensor element in the complex. Considering the increased hyperpolarizability of the complex compared to free sesquifulvalene, it appears that the contribution of these two orbitals with partial sesquifulvalene character remains approximately constant in magnitude upon complex formation. The major part of the contributions to β_{zzz} in **2**, however, arises from the set of three occupied orbitals, labeled 39a′, 26a″, and 40a′, which are predominantly ruthenium d-orbitals in character. As can be seen from Table 5, the combination of two of these occupied orbitals, 39a′ and 40a′, with the unoccupied orbital 41a′, which is mainly located at the seven-membered ring of the sesquifulvalene ligand, accounts for 42% and 19% of the total β_{zzz} of **2**, respectively. Another major contribution of 22%, accounting for the remaining part of β_{zzz}, originates from the ruthenium d-orbital labeled 26a″ in combination with 27a″ (i.e., 26a″ ↔ 27a″), which resembles the LUMO+1 molecular orbital of isolated sesquifulvalene.

In summary, a major part of the hyperpolarizability of the complex can be attributed to the presence of occupied metal d-orbitals according to the present orbital decomposition scheme. In addition, we have demonstrated that more than just HOMO and LUMO have to be considered to account for all contributions of the hyperpolarizability. Hence, our results support the view that the popular two-level formula should only be regarded as a very crude guideline, since important contributions may be missed by relying on it.

To conclude this section, we note that a quantitative agreement among the calculated first hyperpolarizabilities presented here and the experimental Hyper−Rayleigh scattering values reported in ref 17 in general could not be achieved (cf. also ref 44) and is not to be expected either for the following reasons. First, the experimental values have been determined in solution, while the values given here refer to the gas phase. Second, the frequency-dependent first hyperpolarizabilities, at the incident laser wavelength for the Hyper−Rayleigh scattering experiment, are considerably enhanced due to resonance effects. This general problem has been described in considerable detail in ref 17, and may also introduce some uncertainty in the experimental results. More severely, however, resonance-enhanced hyperpolarizability values can be difficult to reproduce theoretically even if frequency-dependent response theory is employed as in the present contribution. The reason is that the frequency-dependent hyperpolarizability exhibits poles at the excitation frequencies of the molecular system under consideration, i.e., if the light frequency approaches a resonance of the molecule, a large change in its hyperpolarizability will result. This enhancement will be larger the closer the photon energy approaches a true excitation energy of the system. In the present case, the relevant photon energies are sufficiently close to excitation energies of the complexes to cause significant resonance enhancement. Hence, rather small deviations of the calculated excitation energies from the true, experimental ones can result in large deviations from the experimentally determined hyperpolarizabilities. Given that present-day TDDFT calculations can do excitations hardly better than 0.3 eV for transition metal complexes (in the gas phase),[45] one should not expect quantitative agreement of first hyperpolarizabilities calculated by TDDFT methods and experiment in the present case.

4. Conclusions and Outlook

In this article, an analysis of the electronic structure and response properties, in particular first hyperpolarizabilities, of sesquifulvalene **1** and a prototype cationic sesquifulvalene ruthenium complex **2** has been given based on time-dependent density-functional response calculations. In fact, the present TDDFT calculations predict an 8-fold increase in the static first hyperpolarizability when **1** is transformed to **2** by complexation with a cationic $[RuCp]^+$ fragment.

To analyze the computed hyperpolarizabilities, a new orbital decomposition scheme for first hyperpolarizabilities has been implemented that allows us to directly relate the (frequency-dependent) first hyperpolarizability tensor elements of any molecule to its electronic structure. The new scheme is based on response theory, is easy to use, and comes at virtually no additional computational cost. The reliability of the scheme has been demonstrated for the standard chromophore *p*-nitroaniline (PNA) by using several basis sets and exchange-correlation potentials.

The electronic structure of the sesquifulvalene ruthenium prototype complex **2** can be understood from the frontier orbitals of the sesquifulvalene ligand (**1**) and the well-known splitting of the d levels in ruthenocene as found in many textbooks. In essence, the three highest occupied orbitals of **2** have dominant d character, while the two lowest unoccupied orbitals are predominantly located on the sesquifulvalene ligand. The low-energy part of the electronic excitation spectrum of **2** is dominated by an intense excitation, which involves a charge transfer from the five-membered rings in **2** to the seven-membered ring of the sesquifulvalene ligand, and at lower energy a somewhat less intensive metal-to-ligand charge-transfer

(MLCT) excitation. The former excitation in **2** is red-shifted compared to the analogous excitation in free sesquifulvalene **1**. This red shift of what is the most intense excitation in both systems might, at first sight, be held responsible for the increased hyperpolarizability of **2** compared to **1**.

An analysis of the computed hyperpolarizabilities, however, reveals a quite different mechanism for the enhancement of the nonlinear optical response of complex **2** with respect to **1**. The hyperpolarizability of sesquifulvalene **1** is not due to the optically intense (HOMO-1) → (LUMO+1) transition, but rather due to the optically "dark" HOMO → LUMO transition. The latter orbital transition can be characterized by a lower energy difference and a higher dipole moment change than the former, which compensates for the lower transition dipole moment of the orbital excitation. The enhanced hyperpolarizability of **2** is predominantly due to a type of transition that has no analogue in free sesquifulvalene, namely a MLCT transition involving an excitation from ruthenium d-orbitals as donors to the seven-membered ring part of the sesquifulvalene ligand. Hence, the effect of complexation of the transition metal fragment $[RuCp]^+$ to sesquifulvalene (**1** → **2**) should not be regarded merely as an enhancement of what is basically the nonlinear optical response of sesquifulvalene. Rather, the NLO activity is changed in an essential manner by introducing new "donor" states, i.e., the ruthenium d-orbitals.

It has been shown that the decomposition scheme has the potential to become a tool that facilitates the directed design of improved chromophores based on existing structures. In the case of sesquifulvalene complexes, the analysis has revealed that the metal d levels play a crucial role as electron donors in the generation of the nonlinear optical response. One manifest strategy toward an improved nonlinear response is therefore to introduce ligands or substituents at selected positions into the basic structure of **2**, which push the d levels of the metal center up in energy and thus reduce the gap between the occupied and unoccupied manifolds. Substitutions at the sesquifulvalene seven-membered ring that lower the LUMO would also be helpful. This and other lines are currently being investigated in our labs.

Acknowledgment. W.H. is grateful for support from the European Commission within the Marie Curie fellowship program (Human Potential Programme, HPMFCT-2000-00678 and MERG-CT-2004-510600). We are also grateful to the National Computing Facilities foundation (NCF) of The Netherlands foundation for Scientific Research (NWO) for a grant of computer time.

References and Notes

(1) Shen, Y.-R. *The Principles of Nonlinear Optics*; Wiley: Hoboken, NJ, 2003.

(2) Boyd, R. W. *Nonlinear Optics*; Academic Press: Amsterdam, The Netherlands, 2003.

(3) Günter, P. *Nonlinear Optical Effects and Materials*, 1st ed.; Schawlow, A. L., Siegman, A. E., Tamir, T., Eds.; Springer: Berlin, Germany, 2000; Vol. 72.

(4) Kanis, D. R.; Ratner, M. A.; Marks, T. J. *Chem. Rev.* **1994**, *94*, 195−242.

(5) Orr, B. J.; Ward, J. F. *Mol. Phys.* **1971**, *20*, 513−526.

(6) Oudar, J. L.; Chemla, D. S. *J. Chem. Phys.* **1977**, *66*, 2664−2668.

(7) Kanis, D. R.; Ratner, M. A.; Marks, T. J. *J. Am. Chem. Soc.* **1992**, *114*, 10338−10357.

(8) Dirk, C. W.; Kuzyk, M. G. *Phys. Rev. A* **1989**, *39*, 1219−1226.

(9) Tomonari, M.; Ookubo, N.; Takada, T.; Feyereisen, M. W.; Almlöf, J. *Chem. Phys. Lett.* **1993**, *203*, 603−610.

(10) Long, N. J. *Angew. Chem., Int. Ed. Engl.* **1995**, *34*, 21−38.

(11) Whittall, I. R.; McDonagh, A. M.; Humphrey, M. G.; Samoc, M. *Adv. Organomet. Chem.* **1998**, *42*, 291−362.

(12) Morley, J. O. *J. Am. Chem. Soc.* **1988**, *110*, 7660−7663.

(13) Nandi, P. K.; Mandal, K.; Kar, T. *Chem. Phys. Lett.* **2003**, *381*, 230−238.

(14) Yang, M.; Jacquemin, D.; Champagne, B. *Phys. Chem. Chem. Phys.* **2002**, *4*, 5566−5571.

(15) Clays, K.; Persoons, A. *Phys. Rev. Lett.* **1991**, *66*, 2980−2983.

(16) Clays, K.; Persoons, A. *Rev. Sci. Instrum.* **1992**, *63*, 3285−3289.

(17) Heck, J.; Dabek, S.; Meyer-Friedrichsen, T.; Wong, H. *Coord. Chem. Rev.* **1999**, *190*−*192*, 1217−1254.

(18) Wong, H.; Meyer-Friedrichsen, T.; Farrell, T.; Mecker, C.; Heck, J. *Eur. J. Inorg. Chem.* **2000**, 631−646.

(19) Meyer-Friedrichsen, T.; Wong, H.; Prosenc, M. H.; Heck, J. *Eur. J. Inorg. Chem.* **2003**, 936−946.

(20) Tamm, M.; Grzegorzewski, A.; Brüdgam, I. *J. Organomet. Chem.* **1996**, *519*, 217.

(21) Tamm, M.; Grzegorzewski, A.; Steiner, T.; Jentzsch, T.; Werncke, W. *Organometallics* **1996**, *15*, 4984−4990.

(22) Tamm, M.; Bannenberg, T.; Baum, K.; Fröhlich, R.; Steiner, T.; Meyer-Friedrichsen, T.; Heck, J. *Eur. J. Inorg. Chem.* **2000**, 1161−1169.

(23) van Gisbergen, S. J. A.; Snijders, J. G.; Baerends, E. J. *J. Chem. Phys.* **1998**, *109*, 10644−10656.

(24) Runge, E.; Gross, E. K. U. *Phys. Rev. Lett.* **1984**, *52*, 997−1000.

(25) Gross, E. K. U.; Kohn, W. *Adv. Quantum Chem.* **1990**, *21*, 255.

(26) Casida, M. E. *Time-Dependent Density Functional Response Theory for Molecules*; Chong, D. P., Ed.; World Scientific: Singapore, 1995; Vol. 1, pp 155−192.

(27) Petersilka, M.; Grossmann, U. J.; Gross, E. K. U. *Phys. Rev. Lett.* **1996**, *76*, 1212.

(28) Gross, E. K. U.; Dobson, J. F.; Petersilka, M. *Density functional theory of time-dependent phenomena*; Nalewajski, R. F., Ed.; Springer: New York, 1996; pp 1−71.

(29) te Velde, G.; Bickelhaupt, F. M.; Baerends, E. J.; Fonseca-Guerra, C.; van Gisbergen, S. J. A.; Snijders, J. G.; Ziegler, T. *J. Comput. Chem.* **2001**, *22*, 931−967.

(30) van Gisbergen, S. J. A.; Snijders, J. G.; Baerends, E. J. *Comput. Phys. Commun.* **1999**, *118*, 119−138.

(31) Ceperly, D. M.; Alder, B. J. *Phys. Rev. Lett.* **1980**, *45*, 566.

(32) Vosko, S. H.; Wilk, L.; Nusair, M. *Can. J. Phys.* **1980**, *58*, 1200.

(33) Grüning, M.; Gritsenko, O. V.; van Gisbergen, S. J. A.; Baerends, E. J. *J. Chem. Phys.* **2001**, *114*, 652−660.

(34) Becke, A. D. *Phys. Rev. A* **1988**, *38*, 3098.

(35) Perdew, J. P. *Phys. Rev. B* **1986**, *33*, 8822.

(36) van Leeuwen, R.; Baerends, E. J. *Phys. Rev. A* **1994**, *49*, 2421.

(37) Hieringer, W.; van Gisbergen, S. J. A.; Baerends, E. J. *J. Phys. Chem. A* **2002**, *106*, 10380−10390.

(38) Sekino, H.; Bartlett, R. J. *J. Chem. Phys.* **1986**, *85*, 976.

(39) Karna, S. P.; Dupuis, M. *J. Comput. Chem.* **1991**, *12*, 487−504.

(40) Langhoff, P. W.; Epstein, S. T.; Karplus, M. *Rev. Mod. Phys.* **1972**, *44*, 602−644.

(41) From the definition given in eq 3 it should be clear that a dominant contribution of a single orbital or a single pair of orbitals does not imply that the contribution originates from these orbitals only (although we will occasionally use the sloppy way of expression). Rather, it means that this contribution would be lost if the given orbital or orbital pair would be left out from the sum.

(42) Ward, J. F. *Rev. Mod. Phys.* **1965**, *37*, 1.

(43) Gritsenko, O. V.; Schipper, P. R. T.; Baerends, E. J. *Chem. Phys. Lett.* **1999**, *302*, 199−207.

(44) Willetts, A.; Rice, J. E.; Burland, D. M. *J. Chem. Phys.* **1992**, *97*, 7590−7599.

(45) Rosa, A.; Ricciardi, G.; Gritsenko, O. V.; Baerends, E. J. *Struct. Bonding* **2004**, *112*, 49−116.